Condensation of actin filaments pushing against a barrier

2011 New J. Phys. 13 103032

(http://iopscience.iop.org/1367-2630/13/10/103032)

New Journal of Physics
The open-access journal for physics

Condensation of actin filaments pushing against a barrier

Kostas Tsekouras[1,2,4], David Lacoste[1], Kirone Mallick[3] and Jean-François Joanny[2]

[1] Laboratoire de Physico-Chimie Théorique—UMR CNRS Gulliver 7083, ESPCI, 10 rue Vauquelin, F-75231 Paris, France
[2] Physico-Chimie UMR 168, Institut Curie, Paris, France
[3] Service de Physique Théorique, Commissariat à l'Energie Atomique-Saclay, Gif, France
E-mail: ktsekouras@ucmerced.edu and tamytes8a@gmail.com

New Journal of Physics **13** (2011) 103032 (16pp)
Received 19 May 2011
Published 24 October 2011
Online at http://www.njp.org/
doi:10.1088/1367-2630/13/10/103032

Abstract. We develop a model to describe the force generated by the polymerization of an array of parallel biofilaments. The filaments are assumed to be coupled only through mechanical contact with a movable barrier. We calculate the filament density distribution and the force–velocity relation with a mean-field approach combined with simulations. We identify two regimes: a non-condensed regime at low force in which filaments are spread out spatially and a condensed regime at high force in which filaments accumulate near the barrier. We confirm a result previously known from other related studies, namely that the stall force is equal to N times the stall force of a single filament. In the model studied here, the approach to stalling is very slow, and the velocity is practically zero at forces significantly lower than the stall force.

[4] Author to whom any correspondence should be addressed.

Contents

1. Introduction

Actin filaments and microtubules are key components of the cytoskeleton of eukaryotic cells. Both play an essential role in cell motility and form the core components of various structures such as lamellipodia or filopodia. They are active elements that exhibit rich dynamic behavior. For instance, actin filaments treadmill in a process where monomers are depolymerized from one end of the filament while other monomers are repolymerized at the other end. Actin polymerization is highly regulated in the cell, through many actin-binding proteins. Some of these proteins accelerate actin polymerization, while others cross-link filaments or create new branches from existing filaments. All these proteins ultimately control the force that a cell is able to produce [1].

Given the complexity of actin polymerization, many studies have focused on its basic structural element, namely the filament itself. For instance, a lower bound for the polymerization force generated by a single actin filament has been deduced from the buckling of a filament that was held at one end by a formin domain and at the other end by a myosin motor [2]. Other studies focused on the dynamics of single filaments through depolymerization experiments [3]. In order to understand the rich dynamical behavior of single filaments such as actin or microtubules and the force they can generate, discrete stochastic models have been developed that incorporate at the molecular level the coupling of hydrolysis and polymerization [4–11]. The filament dynamics and the force generation are two related aspects: hydrolysis is relevant not only for understanding the single-filament dynamics but also for the force generation, since the force generated by a filament is typically lowered by hydrolysis [6].

Ensembles of parallel interacting filaments are able to generate larger forces than single filaments as in cellular structures called filopodia [12]. General thermodynamic principles controlling the force produced by the polymerization of growing filaments pushing against a movable barrier were put forward many years ago by Hill and Kirschner [13]. For many years, however, it was unclear how to extend these results in order to understand theoretically the

effect of interactions or collective effects in the process of force generation. Progress in this direction was made through the introduction of stochastic models for ensembles of parallel microtubules [14–16] and through the development of simulations for actin filaments in parallel geometry [17] or in networks [18]. In these works, the Brownian ratchet model [19] was used at the single-filament level, while some specific rule was assumed concerning the way the load is shared between the filaments. In the absence of hydrolysis and lateral interactions between the filaments, the stall force of an ensemble of parallel N filaments should be N times the stall force of a single filament, as confirmed either by a detailed balance argument valid only near stalling [15] or, more recently, by a more general analysis based on decomposition into cycles [20].

In this paper, we propose a new theoretical framework for this problem. One novel aspect as compared to the previous work [15] comes from the fact that we model the dynamics of an ensemble of parallel non-interacting filaments at an arbitrary value of the force, rather than just predict the value of the stall force. Another important difference between this model and the previous work is that our model allows an arbitrary number of filaments in contact with the moving wall, which allows the possibility of a condensation transition for the number of filaments at the wall.

This paper is organized as follows: we first present the model, then the mean-field approach for the general case of an arbitrary N and finally the simulations and a theoretical analysis of the approach to stalling. We end the paper with a discussion of various related experiments in this field, in which forces generated by a few actin filaments have been measured [21, 22].

2. Model

We consider two rigid flat surfaces: one fixed where filaments are nucleated (nucleating wall) and one movable (barrier) whose position is defined to be the position of the filament(s) furthest away from the nucleating wall (thus there is always at least one filament in contact with the barrier). In the cellular environment, this 'barrier' is often a membrane against which filaments exert mechanical forces. We do not model the internal structure of the filaments, and in particular we do not account for ATP hydrolysis. After nucleation, the filaments grow or shrink by exchanging monomers with the surrounding pool of monomers, which acts as a reservoir. The filaments are coupled only through mechanical contact with the barrier. In some previous models [14], a staggered distribution of initial filaments was assumed so that there would be only a single filament in contact at a time. Here we do not make such an assumption; in contrast, monomers inside different filaments are precisely lined up. As a result, the number of filaments at contact is an arbitrary strictly positive integer.

It follows that we can separate the filaments into two populations, the free filaments that are not in contact with the barrier and the filaments in contact. Only the filaments in contact feel the force exerted by the barrier on them, and as a result, this changes their polymerization rates as compared with free filaments. We assume that a monomer can be added to any free filament with a rate U_0 or removed with a rate W_0, as shown in figure 1. Similarly, a monomer can be added to a filament in contact with a rate $U(F)$, and removed with a rate $W(F)$ (or W_0 as explained below). The values of the rates that we have used correspond to an actin barbed end and are given in table 1. We also assume that the barrier exerts a constant force F on the filaments in contact; this force is defined to be positive when the filaments are compressed.

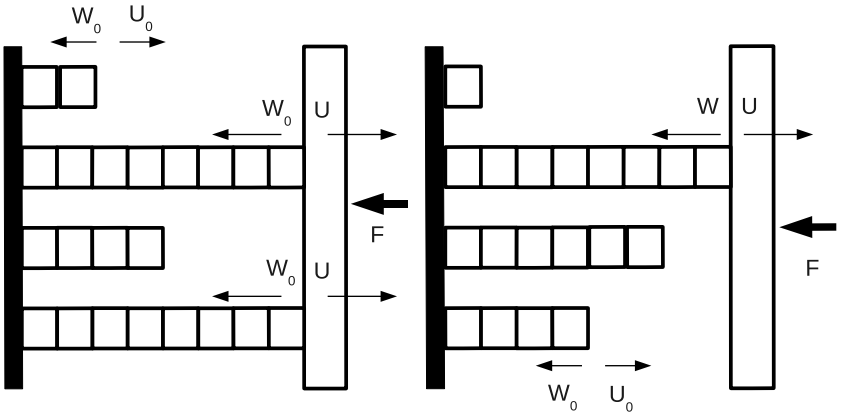

Figure 1. Representation of the filaments pushing on a barrier (the white vertical rectangle on the right, which exerts a force F on the filaments). The right figure corresponds to the case when only one filament is in contact with the barrier, while the left figure corresponds to the case when several filaments are in contact with the barrier. The on- and off-rate of monomers on free filaments are U_0 and W_0. The on-rate on filaments in contact is U, and the off-rate is W if there is only one filament in contact and is W_0 otherwise.

Table 1. Parameters characterizing an actin filament barbed end. W_0 is the free filament depolymerization rate and k_0 is the rate constant entering the free filament polymerization rate $U_0 = k_0 C$, where C is the concentration of free monomers, d is the monomer size and C_c is the critical concentration.

W_0 (s^{-1})	k_0 ($\mu m^{-1} s^{-1}$)	d (nm)	C_c (μm)
1.4	11.6	2.7	0.141

We need now to specify more precisely how the force exerted by the barrier is shared by the filaments in contact. When a monomer is added to a filament in contact, the barrier moves by one unit, but only the filament on which the monomer has been added does work; we therefore treat all the other filaments as free during that step. Similarly, during depolymerization, filaments depolymerize from the barrier with the free depolymerization rate W_0 as long as there is at least one other filament in contact with the barrier, since in this case the depolymerizing filaments do not produce work. The depolymerization occurs with a rate W only when there is a single filament in contact with the barrier. In this case the filament produces work, since its depolymerization leads to the motion of the barrier.

For a filament that has exchanged work with the barrier through addition or loss of monomers, we use a form of local detailed balance that reads

$$\frac{U}{W} = \frac{U_0}{W_0} e^{-f}. \tag{1}$$

This relation is obeyed by the following parameterization of the rates [15, 23, 24]:

$$U = U_0 e^{-f\gamma} \text{ and } W = W_0 e^{f(1-\gamma)}, \tag{2}$$

where γ is the 'load factor' and f is the non-dimensional force $f = Fd/k_BT$, where d is the monomer length. Note that γ itself could be a function of the force; however, in the following we assume that it is just a constant. More elaborate treatments of the load dependence of the transition rates can be found in, for instance, [25].

An essential feature of this model is that although multiple filaments interact with the barrier, when a monomer is added to one of the filaments in contact, it must do work against the entire load. In the classification of [26], this corresponds to a scenario with 'no load sharing'. If the force could be shared by more than one filament or if the monomers in different filaments were not precisely lined up, the above discussion would still apply: in this case a single filament would carry a fraction of the load at a time, and for that filament a similar local detailed balance would hold. In this case, although the stall force would be the same as in the 'no load sharing' scenario, the form of the force–velocity curve would be affected. Such models have been considered in [15, 16, 20, 26], but for simplicity, in the present paper, we focus on the 'no load sharing' model.

3. Theory

In the particular case when there are only two filaments ($N = 2$), the master equation can be solved exactly in terms of the probability that there is a given gap at a given time between the two filaments, as shown in appendix A. Unfortunately, this approach is limited to the $N = 2$ case, because only in that case is there a single gap between the filaments. For $N > 2$, there are many gaps, so in general such an approach quickly becomes as complicated as the one based on the filaments themselves. So instead of looking for an exact solution, we provide in the section below an approximate but accurate mean-field solution for the general case $N > 2$.

3.1. An ensemble of N filaments with N > 2

We recall that the position of the moving barrier coincides with the position of the longest filament, and we define N_i as the number of filament ends which are present at a distance i from the moving barrier. We take the convention that $i = 0$ corresponds to the barrier itself. Since each filament has only one active end and the total number of filaments is fixed at N, we have the condition that $\sum_{i=0} N_i = N$. After a careful account of all possible events that can occur on any filament in a short time interval, we obtain the following master equations:

$$\frac{dN_i}{dt} = (W_0 + UN_0)N_{i-1} + (U_0 + W\delta_{N_0=1})N_{i+1} - (W_0 + U_0 + UN_0 + W\delta_{N_0=1})N_i, \tag{3}$$

$$\frac{dN_1}{dt} = (U_0 + W\delta_{N_0=1})N_2 - (U_0 + W_0 + W\delta_{N_0=1} + UN_0)N_1 + [W_0(1 - \delta_{N_0=1}) + U(N_0 - 1)]N_0, \tag{4}$$

$$\frac{dN_0}{dt} = (U_0 + W\delta_{N_0=1})N_1 - [U(N_0 - 1) + W_0(1 - \delta_{N_0=1})]N_0, \tag{5}$$

where $\delta_{N_0=1}$ represents the probability that there is only a single filament in contact.

In deriving these equations, we have, for instance, implicitly replaced the joint probability to have N_i filament ends at position i and to have only one filament at contact at time t, namely $P(N_i(t) = N_i, N_0(t) = 1)$ by the product of $P(N_i(t) = N_i)$ and $P(N_0(t) = 1)$. In other words,

a mean-field approximation has already been used. A further consequence of this mean-field approximation is that in these equations, $\delta_{N_0=1}$ can be replaced by its time-averaged value, which we call q:

$$q = \langle \delta_{N_0=1} \rangle. \tag{6}$$

The quantity q is a central feature of our model for $N > 2$. All subsequent results and calculations appearing in this paper follow from this mean-field approximation.

At steady state, the lhs of equation (3) is zero. The rhs leads to a recursion valid for $i \geqslant 2$, which can be solved after a few lines of calculations. The solution is

$$N_i = N_2 \exp(-(\mathrm{i}-2)/l), \tag{7}$$

where l is the correlation length (expressed as the number of subunits) given by

$$l = \left[\ln \left(\frac{U_0 + Wq}{W_0 + U N_0} \right) \right]^{-1}. \tag{8}$$

The other two equations (4) and (5), together with the normalization condition, fix N_2, N_1 and N_0. We find that the average number of filaments in contact with the wall N_0 is

$$N_0 = \frac{(U_0 + Wq - W_0)N}{U_0 + U(N-1) + (W - W_0)q}. \tag{9}$$

When $N = 2$, this mean-field solution agrees with the exact solution derived in appendix A with the additional condition that $\gamma = 1$, in which case the on-rate carries all the force dependence. For an arbitrary value of γ, the mean-field solution does not agree with the exact result obtained for $N = 2$. This is as expected, since the mean-field approximation should work well only in the limit of large N.

The average velocity of the moving barrier is

$$V = d(U N_0 - Wq), \tag{10}$$

where the first term within parentheses is the contribution of the filaments in contact polymerizing with a rate U and the second term is the contribution from depolymerizing events of a single filament in contact. We have not found a way of solving in general the self-consistent equation satisfied by q, namely equation (6), except near stalling conditions as explained in the next section. For this reason, we have calculated q numerically from simulations, and derived predictions from the mean-field theory assuming that q is known. For instance, using equations (9) and (10), one obtains the average velocity.

4. Results

4.1. Numerical validation of the mean-field approach

We have tested the validity of the mean-field approach using numerical simulations. We used the classical Gillespie algorithm [27] incorporating the Mersenne Twister random number generator. Runs were executed for N up to 5000. Up to 200 trial runs were used to derive averages and distributions. We validated the simulation results by comparing them with the particular cases $N = 1$ and $N = 2$ for which an exact solution is known (it is given in [6] for $N = 1$ and in the previous section for $N = 2$).

By evaluating the parameter q from the simulations, we obtained very good agreement between the theoretical approach based on the use of mean-field and the simulations for the

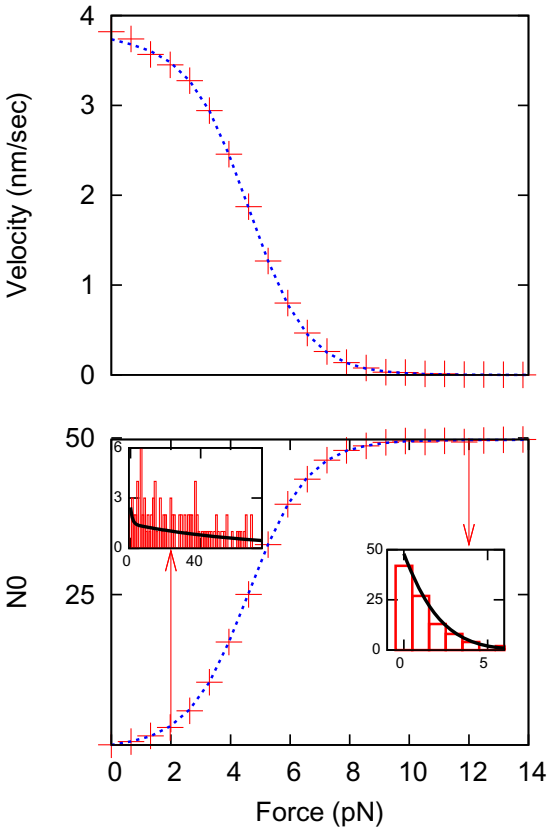

Figure 2. Illustration of the condensation transition of actin filaments against a barrier. Top: average barrier velocity versus force. Symbols represent simulation results; the dotted line represents mean-field predictions based on equation (10). Bottom: average number of filaments in contact with the barrier. Symbols represent simulation results; the dotted line represents mean-field predictions based on equation (9). For both plots, the parameters are $N = 100$, $\gamma = 1$ and $C = 0.24\,\mu$m. Inset, left: density profile in the *non-condensed* regime (bars) as a function of the distance to the barrier, together with mean-field theory prediction (line) from equation (7), for an applied force $F = 2$ pN, which is low with respect to the apparent stall force. Inset, right: density profile in the *condensed* regime (bars) as a function of the distance to the barrier, together with mean-field theory prediction (line) from equation (7), for an applied force $F = 12$ pN, which is close to the apparent stall force of $\approx$12.5 pN.

determination of the force velocity curve (shown in figure 2, bottom) and for the number of filaments N_0 in contact with the barrier (shown in figure 2, top). We find that the values of N_i as determined by theory do not deviate from the simulation value by more than one.

4.2. Condensation transition as a function of the applied force

At low forces, the barrier velocity is close to its maximum value given by the free polymerization velocity. In this case, only one or a small number of filaments are in contact; therefore $q \simeq 1$,

which corresponds to a *non-condensed or single filament* regime. The steady-state density profile of the filaments is broad as shown in figure 2 (bottom, left inset) and the corresponding correlation length is large. With the parameter values corresponding to this figure, we have $l \simeq 151$ nm.

Inversely, at high forces, the filaments accumulate at the barrier. As a result $q \simeq 0$, the density profile is an exponential as shown in figure 2 (bottom, right inset) with a very short correlation length of the order of a monomer size. With the parameter values corresponding to this figure, we have $l \simeq 4.1$ nm. Since in this case, the number of filaments in contact, N_0, is a finite fraction of N, we call this regime the *condensed regime*. In this high force regime (typically near the stall force $F = F_{\text{stall}}$), the following condition is obeyed: $NU \ll U_0$. Since we also have $q \simeq 0$, equation (9) simplifies to

$$N_0 = \left(1 - \frac{W_0}{U_0}\right) N. \tag{11}$$

This equation can be used to predict the finite fraction of filaments in contact in the condensed regime. This condensed regime corresponds to the plateau in the curve of N_0 versus F which is shown in figure 2 (top inset). In the conditions of this figure, equation (11) predicts a plateau for $N_0 \simeq N/2 = 50$ which is indeed observed, and as expected the plateau in N_0 (figure 2, top) occurs at the same force at which the velocity approaches zero (figure 2, bottom).

4.3. Theoretical stall force

Let us first discuss here the theoretical expression for the stall force and then in the next section the practical way this limit is approached. The stall force is defined as the value of the force applied on the barrier for which the velocity given by equation (10) vanishes. For $N = 1$, the stall force is $F^{(1)}_{\text{stall}} = k_{\text{B}}T \ln(U_0/W_0)/d$. For $N = 2$, using the results obtained in appendix A for N_0 and q, we find that the stall force $F^{(2)}_{\text{stall}}$ is exactly twice the stall force of a single filament, $F^{(1)}_{\text{stall}}$,

$$F^{(2)}_{\text{stall}} = 2F^{(1)}_{\text{stall}} = 2\frac{k_{\text{B}}T}{d} \ln\left(\frac{U_0}{W_0}\right). \tag{12}$$

In the general case of an arbitrary number of filaments N, we expect that the stall force $F^{(N)}_{\text{stall}}$ should be [15, 16]

$$F^{(N)}_{\text{stall}} = N\frac{k_{\text{B}}T}{d} \ln\frac{U_0}{W_0}. \tag{13}$$

This result can be derived from the following argument: near stalling conditions, the average density of filaments at contact N_0/N can be obtained from equation (11) above. This average density of filaments can be used as an approximation of the probability of having one filament in contact when $N_0/N \ll 1$. Since q is the probability that there is a single filament in contact (in other words, there is one filament among N in contact and the remaining $N-1$ are free), it follows that

$$q = \binom{N}{1} \frac{N_0}{N} \left(1 - \frac{N_0}{N}\right)^{N-1}, \tag{14}$$

which leads, using equation (11), to

$$q = N\left(1 - \frac{W_0}{U_0}\right)\left(\frac{W_0}{U_0}\right)^{N-1} \simeq N_0 \left(\frac{W_0}{U_0}\right)^{N-1}. \tag{15}$$

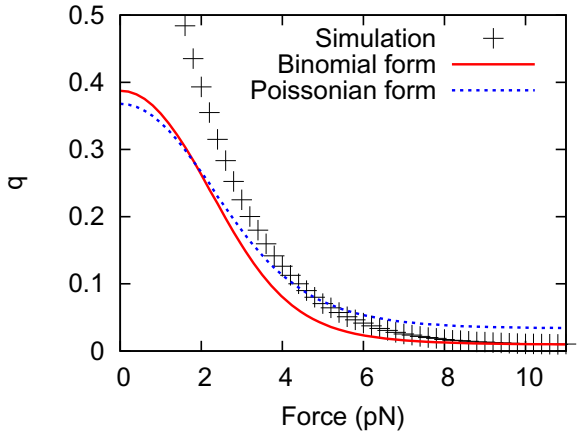

Figure 3. Comparison between the theoretical and numerical estimates for the parameter q, which represents the probability that there is a single filament in contact. Symbols represent simulation results, the dotted line corresponds to equation (16) and the continuous line corresponds to equation (14) (both expressions are mean-field approximations valid in the high force regime). The parameters are $N = 10$, $\gamma = 1$ and $C = 0.24\,\mu$m.

We call this the binomial form for q. We note that equation (14) also means that

$$q \simeq N_0 \exp(-N_0), \tag{16}$$

which corresponds to a Poisson statistics for the distribution of the number of filaments at contact. Now inserting the final expression for q of equation (15) into the stalling condition, namely the vanishing of the velocity given by equation (10), one obtains the theoretical stall force given in equation (13).

The theoretical expression for the stall force given by equation (13) has also been obtained in a recent study devoted to the stall force of a bundle of filaments [20]. This study is based on the model introduced in [14, 15], which the authors modified to include lateral interactions between the filaments of the bundle. Using a theoretical argument based on the identification of relevant polymerization cycles, the authors of [20] confirm the expression for the stall force obtained before in [15], which is also our equation (13). More importantly, they show with this method that this expression has a universal character for models of this kind, hence in particular the independence of the stall force with respect to the load distribution factor γ. They also obtained force velocity curves for various values of the lateral interaction and staggering distance, which—as we have checked—agree with the numerical results obtained in this paper when there is no lateral interaction and when the shifts are zero.

In figure 3, the value of q determined from the simulations is compared with the theoretical expression given by equation (14) or equation (16) (both expressions give similar results). We note that the deviation between the simulation points and the theory increases as the force is lowered; this is due to the mean-field nature of the theory, which becomes invalid when the force is small, since then the fluctuations are large. For completeness, we also show in figure 4 the probability density function of the number of filaments at contact for various forces.

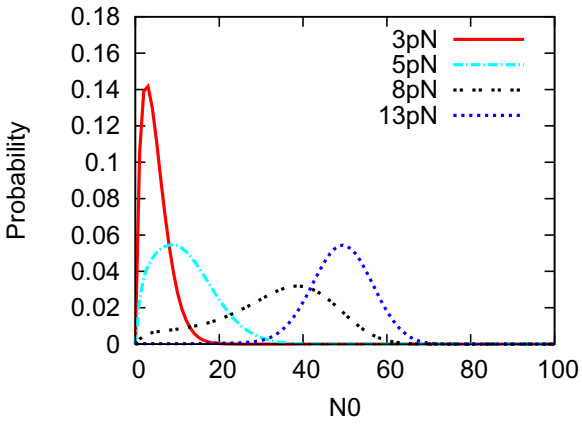

Figure 4. Probability distributions of the number of filaments in contact with the barrier at various forces. The parameters are $N = 100$, $\gamma = 1$ and $C = 0.24\,\mu$m.

4.4. The approach to stalling

Let us now discuss more precisely how the velocity approaches zero. We find that in our simulations, for N larger than about 10, the velocity approaches zero at forces significantly lower than the stall force as shown in figure 2 (bottom). We note that a similar effect has been obtained when analyzing the stall force of an ensemble of interacting molecular motors [28]. To quantify this effect, we therefore define an *apparent* stall force as the value of the force where the velocity drops to less than a small fraction $\alpha = 2.5\%$ of the value it has for zero force [26]. In the experimental situation, this bound could correspond, for instance, to the limit of resolution in the velocity measurement.

The value of the velocity at zero force corresponds to the maximum velocity. When $F = 0$, there is no coupling between the filaments, which behave as independent random walkers. The probability of having more than one walker at the leading position is zero in the long-time limit, which implies $q = 1$. Therefore, $N_0 = 1$ and the velocity at zero force equals the polymerization velocity of a single filament:

$$V(F = 0) = d(U_0 - W_0), \tag{17}$$

which is mainly controlled by the monomer concentration. Now by using the expression for the velocity at an arbitrary force given by equation (10), the expression for N_0 given in equation (9) and the parameterization of the rates of equation (2) for the particular case $\gamma = 1$, we find that

$$F_{\text{app}}^{(N)} = \frac{k_{\text{B}}T}{d} \ln \frac{(1-\alpha)(U_0 - W_0)N + \alpha U_0 - (\alpha - q)W_0}{\alpha U_0 - (\alpha - q)W_0}. \tag{18}$$

Since $q \ll 1$ near stalling, we can write the following more explicit expression:

$$F_{\text{app}}^{(N)} \simeq \frac{k_{\text{B}}T}{d} \ln\left(1 + \frac{N}{\alpha} - N\right). \tag{19}$$

In figure 6, we show the apparent stall force given by equation (18) as a function of N together with the theoretical stall force of equation (13).

Let us show now that filament condensation at the barrier and the drop in velocity occur simultaneously. Assuming for simplicity that $\gamma = 1$, $N \gg 1$ and $q \simeq 0$ in the high force regime,

we can substitute equation (19) into equation (9) to obtain

$$N_0 = (1-\alpha)\left(1-\frac{W_0}{U_0}\right)N. \tag{20}$$

From this we see that since $\alpha \ll 1$, the maximum number of filaments at the barrier is almost reached. If V_0 is the initial velocity and N_0^s is the finite fraction of filaments at the barrier at the stall force, we have the equivalence of the following two conditions:

$$V = \alpha V_0 \Leftrightarrow N_0 = (1-\alpha)N_0^s,$$

which shows that filament condensation occurs at the value of the apparent stall force, a point that is confirmed by simulations. Indeed, in the case of figure 6 the apparent stall force is about 12.7 pN, and the condensation visible in figure 2 also occurs close to 12 pN.

Close to the stall force it is also possible to derive an analytic expression for the force–velocity relation by substituting into equation (10) the expressions of q, given by equations (14) and (16). Assuming for simplicity $\gamma = 1$ and using equation (11), we obtain with the binomial form:

$$V = N\left(1-\frac{W_0}{U_0}\right)\left[U_0\,\mathrm{e}^{-f} - W_0\left(\frac{W_0}{U_0}\right)^{N-1}\right], \tag{21}$$

and with the Poissonian form:

$$V = N\left(1-\frac{W_0}{U_0}\right)\left(U_0\,\mathrm{e}^{-f} - W_0\,\mathrm{e}^{-N(1-W_0/U_0)}\right). \tag{22}$$

When these expressions are expanded close to the stall force, one obtains in both cases

$$\delta V = N\left(1-\frac{W_0}{U_0}\right)U_0\,\mathrm{e}^{-f}\delta f. \tag{23}$$

This indicates an exponential dependence of the velocity close to stalling, which is indeed present in the simulations as shown in figure 5.

To summarize, we have shown in this section that the apparent stall force does not scale linearly with N as the theoretical stall force but rather as $\ln(N)$. The apparent stall force is the quantity of experimental interest; it is also near the apparent stall force that the condensation transition discussed in a previous section occurs (nothing special of that sort occurs near the theoretical stall force).

4.5. Related experimental work in connection with the model

In this section, we discuss related experimental work. Although a precise comparison with the present model is not attempted, we hope that the discussion could be useful in identifying some relevant questions in this field. The force generation by parallel actin filaments growing out of an acrosome bundle has been measured in [21]. The observation of a plateau in force measurements by optical tweezers is a good indication of the stalling regime, but the measured stall force is very small, comparable with that of a single filament, although many filaments are present (about a dozen). These results thus stand at odds with the theoretical predictions for the stall force obtained in [15, 20] (and in the present paper). In the present paper, we have emphasized the fact that the approach to stalling is slow, which can lead to an underestimation of the true stall force. The resolution of the optical tweezers leads to a limit in the detection

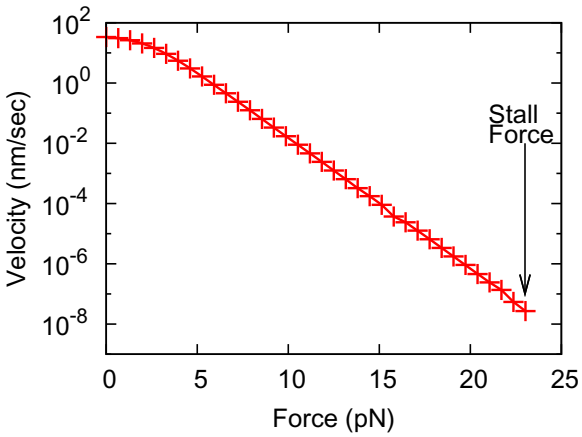

Figure 5. Average barrier velocity on the logarithmic scale as a function of the force in the linear scale. Note that the velocity decreases to near zero exponentially when approaching the theoretical stall force, which is shown by the arrow. For this value of the force, the numerical velocity is not strictly zero, but is close to the uncertainty intrinsic to the simulation, which is here of the order of 10^{-8} nm s^{-1}. The parameters are $N = 10$, $\gamma = 1$ and $C = 1.2\,\mu$m.

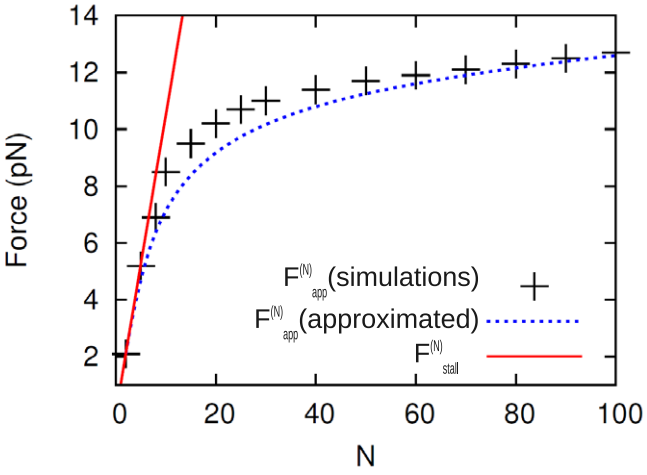

Figure 6. Theoretical stall force $F^{(N)}_{\text{stall}}$ (straight line; calculated from equation (13)) and apparent stall force, both as computed from simulations $F^{(N)}_{\text{simulations}}$ (black symbols) and from the mean-field approximation given in equation (18) $F^{(N)}_{\text{approximated}}$ (dotted line) versus the number of filaments N. The parameters are $\gamma = 1$ and $C = 0.24\,\mu$m.

of small velocities, which corresponds roughly to the criterion for the apparent stall force used in the previous section. However, with a dozen filaments, the apparent stall force should be significantly larger than that of a single filament. Another difficulty is that there is no indication in this experiment of the two regimes of low and large forces discussed in this paper. At this point, it may be important to say that the results of this experiment have not been reproduced; in fact in a new experiment discussed below, where the force generated by filaments growing from

two magnetic beads outwards, very different results have been obtained [22]. In view of all this, we think that the reason for these discrepancies may be found in effects which are not accounted for (such as buckling or filament cross-linking) or they may be attributed more simply to the fact that the two experiments have been done in very different biochemical conditions. Indeed, the authors of [21] have used profilin to suppress spontaneous nucleation of actin filaments, while profilin was absent in [22]. The use of profilin in [21] introduced complications, since profilin also modifies the thermodynamics of the system by binding to actin monomers and possibly interferes with ATP hydrolysis during polymerization.

The mechanical response of an actin network confined between two rigid flat surfaces has been probed using a surface force apparatus (SFA) in [29] and using an atomic force microscope (AFM) in [30]. Both experiments reported a load history-dependent mechanical response, which presumably reflects a complex interplay between buckling and polymerization forces. This complex interplay makes it difficult to isolate the true contribution of polymerization forces. More recently, Brangbour *et al* [22] devised a new experimental setup in which actin is nucleated from magnetic beads that are covered by gelsolin. A magnetic field is used to counteract the polymerization force, which allows one to measure the force–velocity curves. As mentioned above, the results of [21] for the stall force of a single filament are not confirmed: in contrast, the stall force that is obtained is of the order of 40 pN, which corresponds according to equation (13) to about 25 active filaments. The general shape of these force–velocity curves is similar to those obtained in this work, but some deviations are present at low and high forces. These discrepancies suggest that our model may be too simple to fully explain this experiment and that other aspects may be important. Firstly, it would be necessary to go beyond the parallel organization of the filaments in order to better model the experimental geometry of [22]. Secondly, it is probably important to account in the model for the possibility of nucleating new filaments from existing ones [31]. Thirdly, buckling forces could play an important role in the experiment. Some of these effects have been included in previous numerical simulations of branched actin networks [18, 32], but they are typically difficult to study with analytical models of the kind presented here.

5. Conclusion

In this paper, we have provided a new theoretical framework to describe the dynamics of an ensemble of N parallel filaments with no lateral interactions, which are exerting a force against a movable barrier. The special cases $N = 1$ and $N = 2$ can be solved exactly, unlike the general case for arbitrary N, for which we have constructed a mean-field approach. We identify two regimes: a non-condensed regime at low force in which filaments are spread out spatially and a condensed regime at high force in which filaments accumulate near the barrier. The transition occurs near the apparent stall force where the velocity approaches zero. We find that for large N this regime where the velocity approaches zero occurs at forces significantly lower than the theoretical stall force, given by N times the stall force of one filament. In fact, the apparent stall force does not scale linearly with N as the theoretical stall force does; instead it scales logarithmically.

On the theory side, several extensions of our work are worth investigating. For instance, bundles can be formed experimentally by growing filaments in the presence of specific proteins which cross-link the filaments. To describe such a situation, it would be necessary to include lateral interactions. Another direction would be to explore the role of load sharing, as was done

in [26] for instance. Although the dynamics will be different, we still expect a condensation transition to be present in this case.

In the end, our model offers a very simplified view of the problem of force generation by actin filaments, but precisely for this reason we hope that it can be a useful starting point for more refined studies.

Acknowledgments

We thank A B Kolomeisky, P Sens and R Pandinhateeri for stimulating discussions and J Baudry for a careful reading of the manuscript. KT thanks J Elgeti for his help with computational issues. This work was supported by the ANR (the French National Research Agency) under contract no. ANR-09-PIRI-0001-02.

Appendix. Exact solution of the master equation for the case $N = 2$

For this problem, we can derive the following master equation satisfied by $p(n, t)$ the probability that there is a gap of n monomers between the two filaments. For $n > 2$,

$$\frac{\partial p(n,t)}{\partial t} = (U + W_0)[p(n-1,t) - p(n,t)] + (W + U_0)[p(n+1,t) - p(n,t)], \tag{A.1}$$

and otherwise,

$$\frac{\partial p(1,t)}{\partial t} = 2(U + W_0)p(0,t) - (U + W_0)p(1,t) + (W + U_0)[p(2,t) - p(1,t)], \tag{A.2}$$

$$\frac{\partial p(0,t)}{\partial t} = (W + U_0)p(1,t) - 2(U + W_0)p(0,t). \tag{A.3}$$

Solving equation (A.1) at steady state results in the recursion

$$(W + U_0)p(n+1) - (U + W + U_0 + W_0)p(n) + (U + W_0)p(n-1) = 0,$$

which yields two solutions, namely 1 and $b = \frac{U+W_0}{W+U_0}$. This means that for $n \geqslant 2$, $p(n) = p(2)b^{n-2}$.

Using the normalization condition: $p(0) + p(1) + \sum_{n\geqslant 2} p(2)b^{n-2} = 1$, we obtain $p(2) = (1-b)(1-p(0)-p(1))$. Solving equation (A.3) at steady state results in

$$p(1) = 2p(0)\frac{U + W_0}{W + U_0} = 2p(0)b.$$

Substituting this expression into equation (A.2) at steady state yields

$$p(2) = 2p(0)b^2.$$

Equating the two expressions for $p(2)$ and using the expression for $p(1)$ in terms of $p(2)$, it follows that

$$p(0) = \frac{1-b}{1+b}.$$

The probability of having a gap of zero monomers is the probability of having both filaments at the barrier; it thus obeys $p(0) + q = 1$, since q is the probability of having only one filament at the barrier. In the end, we find that

$$q = \frac{2(U + W_0)}{U + W + U_0 + W_0}. \tag{A.4}$$

The average number of filaments at the barrier is the sum of q plus twice $1-q$, since $1-q$ is the probability of having both filaments at the barrier. Therefore

$$N_0 = q + 2(1-q) = 2-q,$$

and if we substitute q from above, we find that

$$N_0 = \frac{2(W+U_0)}{U+W+U_0+W_0}. \tag{A.5}$$

References

[1] Pollard T D and Cooper J A 2009 Actin, a central player in cell shape and movement *Science* **326** 1208–12

[2] Kovar R D and Pollard T D 2004 Insertional assembly of actin filament barbed ends in association with formins produces piconewton forces *Proc. Natl Acad. Sci. USA* **41** 14725–30

[3] Kueh H Y and Mitchison T J 2009 Structural plasticity in actin and tubulin polymer dynamics *Science* **325** 960–3

[4] Stukalin E B and Kolomeisky A B 2005 Polymerization dynamics of double-stranded biopolymers: chemical kinetic approach *J. Chem. Phys.* **122** 104903

[5] Stukalin E B and Kolomeisky A B 2006 ATP hydrolysis stimulates large length fluctuations in single actin filaments *Biophys. J.* **90** 2673–85

[6] Ranjith P, Lacoste D, Mallick K and Joanny J-F 2009 Nonequilibrium self-assembly of a filament coupled to ATP/GTP hydrolysis *Biophys. J.* **96** 2146–59

[7] Ranjith P, Lacoste D, Mallick K and Joanny J-F 2010 Role of ATP-hydrolysis in the dynamics of a single actin filament *Biophys. J.* **98** 1418–27

[8] Vavylonis D, Yang O and O'Shaughnessy B 2005 Actin polymerization kinetics, cap structure, and fluctuations *Proc. Natl Acad. Sci. USA* **102** 8543–8

[9] Antal T, Krapivsky P L, Redner S, Mailman M and Chakraborty B 2007 Dynamics of an idealized model of microtubule growth and catastrophe *Phys. Rev.* E **76** 041907

[10] Antal T, Krapivsky P L and Redner S 2007 Dynamics of microtubule instabilities *J. Stat. Mech.* L05004

[11] Li X, Lipowsky R and Kierfeld J 2010 Coupling of actin hydrolysis and polymerization: reduced description with two nucleotide states *Eur. Phys. Lett.* **89** 38010

[12] Wirtz D, Altigan E and Sun S X 2006 Mechanics and dynamics of actin-driven thin membrane protrusions *Biophys. J.* **90** 65–76

[13] Hill T L and Kirschner M W 1981 Subunit treadmilling of microtubules or actin in the presence of cellular barriers: possible conversion of chemical free energy into mechanical work *Proc. Natl Acad. Sci. USA* **79** 490–4

[14] Mogilner A and Oster G 1999 The polymerization ratchet model explains the force–velocity relation for growing microtubules *Eur. Biophys. J.* **28** 235–42

[15] Sander van Doorn G, Tanase C, Mulder B M and Dogterom M 2000 On the stall force for growing microtubules *Eur. Biophys. J.* **20** 2–6

[16] Tanase C 2004 Physical modeling of microtubule force generation and self-organization *PhD Thesis* Wageningen University

[17] Vavylonis D and O'Shaughnessy B 2006 Brownian ratchet model of force generation and kinetics of actin filament bundles *50th Annual Meeting of the Biophysical Society (Salt Lake City, 18–22 February 2006)*

[18] Carlsson A E 2003 Growth velocities of branched actin networks *Biophys. J.* **84** 2907–18

[19] Peskin C S, Odell G M and Oster G F 1993 Cellular motions and thermal fluctuations: the Brownian ratchet *Biophys. J.* **65** 316–24

[20] Krawczyk J and Kierfeld J 2011 Stall force of polymerizing microtubules and filament bundles *Europhys. Lett.* **93** 28006

[21] Footer M J, Kerssemakers J W J, Theriot J A and Dogterom M 2006 Direct measurement of force generation by actin filament polymerization using an optical trap *Proc. Natl Acad. Sci. USA* **104** 2181–6
[22] Brangbour C, du Roure O, Helfer E, Démoulin D, Mazurier A, Fermigier M, Carlier M-F, Bibette J and Baudry J 2011 Force velocity measurements of a few growing actin filaments *PLoS Biol.* **9** e1000613
[23] Hill T L 1987 *Linear Aggregation Theory in Cell Biology* (Berlin: Springer)
[24] Bell G I 1978 Models for the specific adhesion of cells to cells *Science* **200** 618–27
[25] Walcott S 2008 The load dependence of rate constants *J. Chem. Phys.* **128** 215101
[26] Schaus T E and Borisy G G 2008 Performance of a population of independent filaments in lamellipodial protrusion *Biophys. J.* **95** 1393–411
[27] Gillespie D T 1976 A general method for numerically simulating the stochastic time evolution of coupled chemical reactions *J. Comput. Phys.* **22** 403–34
[28] Campás O, Kafri Y, Zeldovich K B, Casademunt J and Joanny J-F 2006 Collective dynamics of interacting molecular motors *Phys. Rev. Lett.* **97** 038101
[29] Greene G W, Anderson T H, Zen H, Zappone B and Israelachvili J N 2008 Force amplification response of actin filaments under confined compression *Proc. Natl Acad. Sci. USA* **106** 445–9
[30] Fletcher D 2005 Loading history determines velocity of actin network growth *Nat. Cell Biol.* **7** 1219–23
[31] Achard V, Martiel J-L, Michelot A, Guerin C, Reymann A-C, Blanchoin L and Boujemaa-Paterski R 2010 A primer-based mechanism underlies branched actin filament network formation and motility *Curr. Biol.* **20** 423–8
[32] Lee K-C and Liu A J 2009 Force–velocity relation for actin-polumerization-driven motility from Brownian dynamics simulations *Biophys. J.* **97** 1295–304